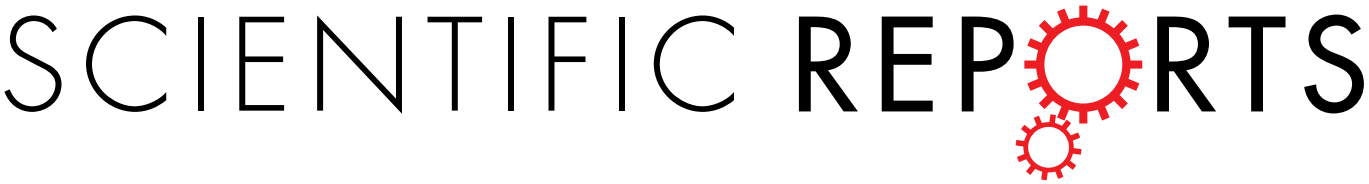

OPEN

Heterogeneous Nucleation of Trichloroethylene Ozonation Products in the Formation of New Fine Particles

Received: 19 October 2016
Accepted: 11 January 2017
Published: 15 February 2017

Ning Wang[1], Xiaomin Sun[1], Jianmin Chen[2] & Xiang Li[2]

Free radicals in atmosphere have played an important role in the atmospheric chemistry. The chloro-Criegee free radicals are produced easily in the decomposition of primary ozonide (POZ) of the trichloroethylene, and can react with O_2, NO, NO_2, SO_2 and H_2O subsequently. Then the inorganic salts, polar organic nitrogen and organic sulfur compounds, oxygen-containing heterocyclic intermediates and polyhydroxy compounds can be obtained. The heterogeneous nucleation of oxidation intermediates in the formation of fine particles is investigated using molecular dynamics simulation. The detailed nucleation processes are reported. According to molecular dynamics simulation, the nucleation with a diameter of 2 nm is formed in the Organic Compounds-$(NH_4)_2SO_4$-H_2O system. The spontaneous nucleation is an important process in the formation of fine particles in atmosphere. The model study gives a good example from volatile organic compounds to new fine particles.

Atmospheric organic aerosols have enormous and remarkable impact on the global climate. They influence the formation and lifetime of clouds, and affect the concentration of gas phase species as these species can react on aerosols' surfaces[1]. Secondary organic aerosols (SOA) account for approximately 10% of the total organic aerosol loadings and up to 90% of organic aerosols in urban environments[2].

The ozonolysis of alkenes is an important reaction in atmospheric chemistry, and ozonolysis intermediates-Criegee Intermediates (CIs) can be generated in this progress[3,4]. CIs will further generate the secondary ozonide (SOZ), which can make significant contribution to SOA mass, a significant source of SOA in the troposphere[5–10].

Previous studies suggest that aerosols, fog, and cloud water may play a key role in the atmospheric chemistry[11–13]. In-cloud SOA formation is likely to enhance organic PM concentrations in the free troposphere and organic aerosol concentrations in locations, and leads to serious pollution in the atmospheric environment. There are several significant atmospheric events, such as London Fog mainly emanated by SO_2 from coal burning[14], Los Angeles Smog caused by NOx and VOCs from traffic emissions[15–17], Beijing Haze co-initiated by SO_2, NOx and VOCs[18–20]. One of the most important properties is the high level of particulate matter which profoundly impacts human health, visibility, the ecosystem, weather and climate[21,22].

So far, the mechanisms of PM formation remain uncertain in detail, especially for microscopic mechanism of the processes related to PM origin and growth[2,23–26]. A few theoretical researches focuses on PM formation mechanism which involves many chemical constituents of organic and elemental carbon, sulfate, nitrate, ammonium and trace metals carbon.

It is well known that oxidants play a crucial role in atmospheric chemistry processes. Free radicals produced by the olefin's ozonation become a major kind of atmospheric oxidants which is key to the formation of fine particles, and has drawn great attention[27–30].

Trichloroethylene (TCE), as a kind of chloroethylenes, is one of the most important volatile organic compounds (VOCs)[31,32]. TCE is a contaminant as it is highly toxic, carcinogenic, when it is released into the atmosphere and subsurface of groundwater[33–35].

[1]Environment Research Institute, Shandong University, Jinan 250100, P. R. China. [2]Department of Environmental Science and Engineering, Fudan University, China. Correspondence and requests for materials should be addressed to X.S. (email: sxmwch@sdu.edu.cn) or X.L. (email: lixiang@fudan.edu.cn)

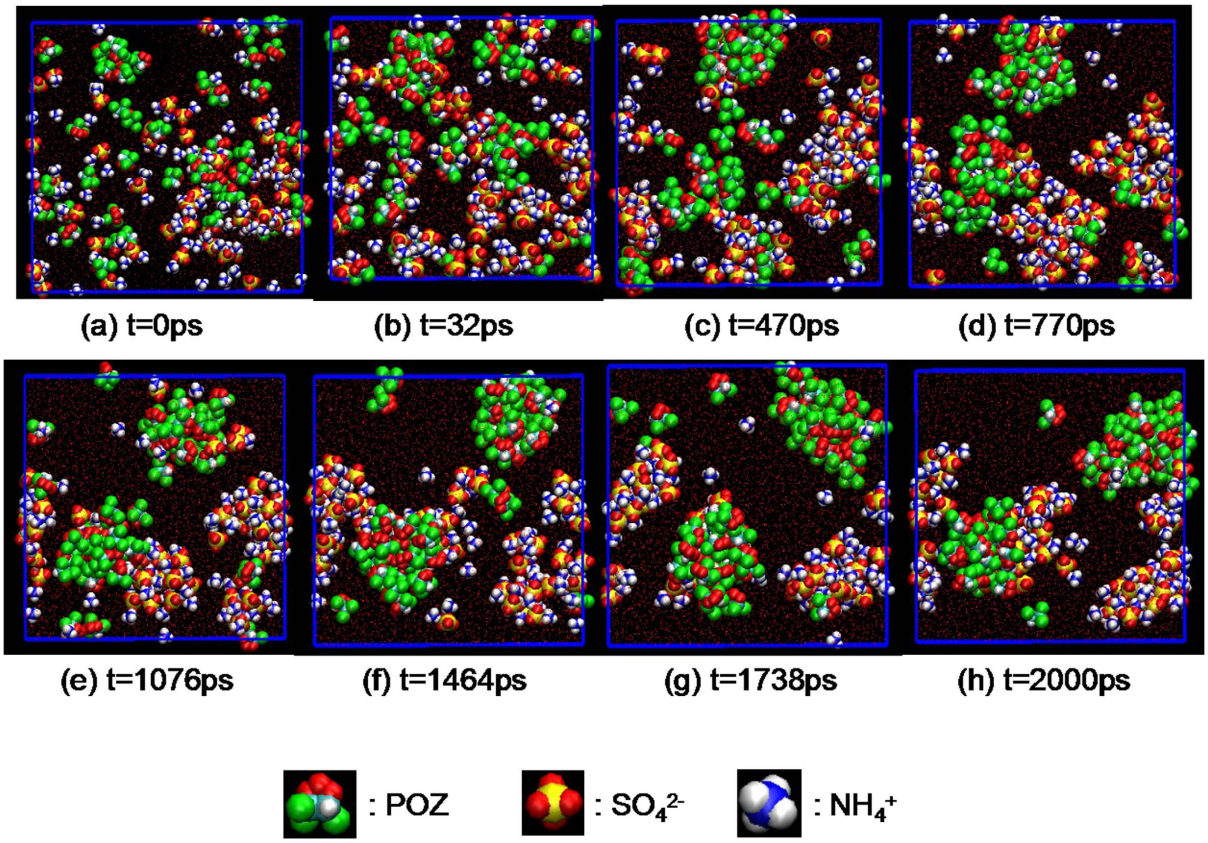

Figure 1. The snapshot of distribution of the equilibrium configuration in the POZ-$(NH_4)_2SO_4$-H_2O system at different time.

In the ozonolysis process of TCE, a primary ozonide (POZ) is produced. It is a cyclic compound and will decompose into two kinds of CI (i.e., IM1 and IM2), phosgene and formyl chloride, eventually produce two kinds of SOZ (i.e., SOZ1 and SOZ2). SOZ can make significant contribution to SOA mass.

In this paper, the oxidation intermediates of chlorinated Criegee radicals produced in trichloroethylene ozonation on the heterogeneous nucleation of the fine particles is under investigation using molecular simulation. The molecular dynamics simulation will be performed to study nucleation in the OCs-$(NH_4)_2SO_4$-H_2O system, which is an important process in the formation of fine particles in atmosphere.

Results

The new particle formation. Many polar intermediates will be formed in the process of trichloroethylene ozonation, such as POZ, SOZ*i* ($i = 1–2$), IM*i* ($i = 1–20$), and P*i* ($i = 1–14$) (See Supplementary Fig. S1-S3). These species will participate in the nucleation of new particles or the formation of secondary organic aerosols through their own aggregation or absorbing fine particles in the atmosphere. The systems consisting of above typical Organic Compounds(OC), $(NH_4)_2SO_4$, and H_2O are chosen as an example to study equilibrium distributions of individual particles using molecular dynamics simulation and to further probe the formation of new fine particles. The typical OCs are POZ, SOZ1, IM6, IM11, P2, P3, P6, P7 and P10.

Distribution of equilibrium configurations. The snapshots of POZ-$(NH_4)_2SO_4$-H_2O system at different time are discussed as an example in Fig. 1. At $t = 0$ ps, there is no obvious nucleation and the particles are dispersed uniformly. With simulation time increasing, nucleation phenomenon is more and more evident. When the system reaches equilibrium, both POZ and $(NH_4)_2SO_4$ have a nucleus solely and larger clusters through their absorption of each other. Other systems reveal the similar phenomenon, and snapshots for the distribution of equilibrium configuration (see Supplementary Fig. S4–S12). Each system can form clusters of different sizes, *i.e.*, different nucleus, including inter- and intra- nucleation of the $(NH_4)_2SO_4$ and OCs. The diameter of the nucleation clusters is about 2 nm.

Radial distribution function. For further data analysis, the radial distribution function of those particles can be obtained from the thermodynamic equilibrium system. The Radial distribution function *g (r)* is a reflection on the physical characteristics of the fluid microstructure, which indicates a probability of another molecule density around a molecule at a distance *r* where the ratio is randomly distributed with respect to the probability density.

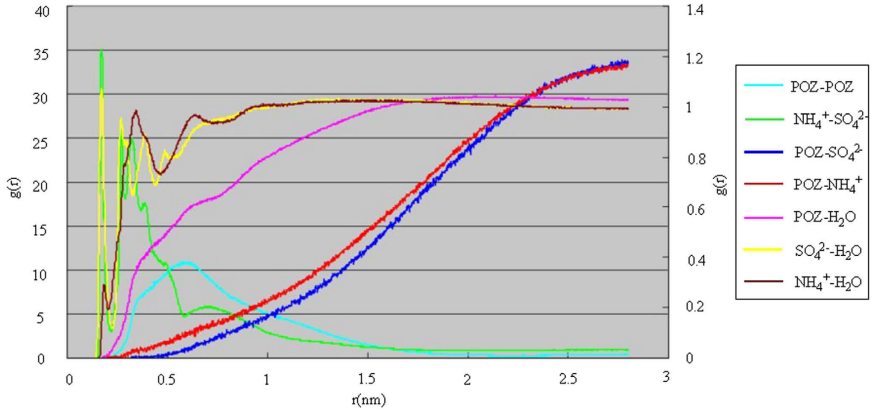

Figure 2. The radial distribution functions for the main particles in the POZ-$(NH_4)_2SO_4$-H_2O system.

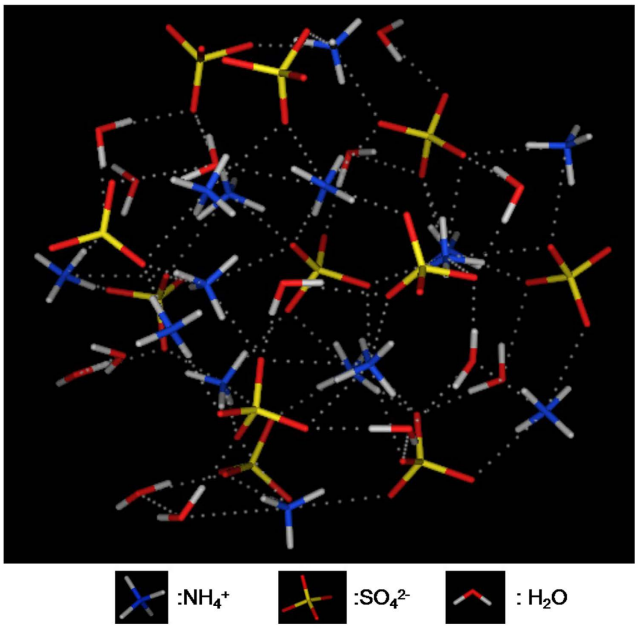

Figure 3. The bonding mode of SO_4^{2-} with other particles around 0.5 nm in the POZ-$(NH_4)_2SO_4$-H_2O system.

$$g(r) = \rho(r)/\rho$$

where $\rho(r)$ is the local density from the center of molecule r to the volume element dr, and ρ is the average density.

The radial distribution functions for main particles in the POZ-$(NH_4)_2SO_4$-H_2O system are suggested in Fig. 2. It is obvious that the radial distribution function curve of NH_4^+ and SO_4^{2-} have two distribution peaks around 0.21 nm and 0.35 nm, mainly due to electrostatic interactions between NH_4^+ and SO_4^{2-}. In the RDF curve of NH_4^+ and H_2O, there are two peaks about 0.35 nm and 0.61 nm too. The first peak is mainly resulted from the static electricity of NH_4^+ and H_2O and the hydration structure (*i.e.*, the first hydration layer) could be generated. And the second peak comes from hydrogen bonds between the first hydration structure and other water to form the new hydration structure (*i.e.*, the second hydration layer). The RDF curve of SO_4^{2-} and H_2O is similar to that of NH_4^+ and H_2O. The main difference lies in that peaks occur at smaller distance regions, which may be due to stronger Coulomb interaction between SO_4^{2-} and H_2O. Then the stronger Coulomb interaction can help the inner hydration layer water take effect with other water to produce the second and third hydration layer through hydrogen bonds. There are three distinct peaks in the RDF curve of SO_4^{2-} and H_2O. There is a clear and broad peak at 0.6 nm in the RDF curve of POZ and POZ, indicating the presence of nucleation between organic molecules. It can be found that the RDF curves of POZ and SO_4^{2-}, NH_4^+, H_2O have a monotonously rising trend, which indicates that there is no obvious aggregation between POZ and SO_4^{2-}, NH_4^+, H_2O. In addition, the RDF curves of POZ and H_2O are steeper than those of POZ and SO_4^{2-}, NH_4^+. So the water molecules begin to have a significant position in distribution at a distance of 0.5–1.5 nm around POZ, while SO_4^{2-}, NH_4^+ at a distance of

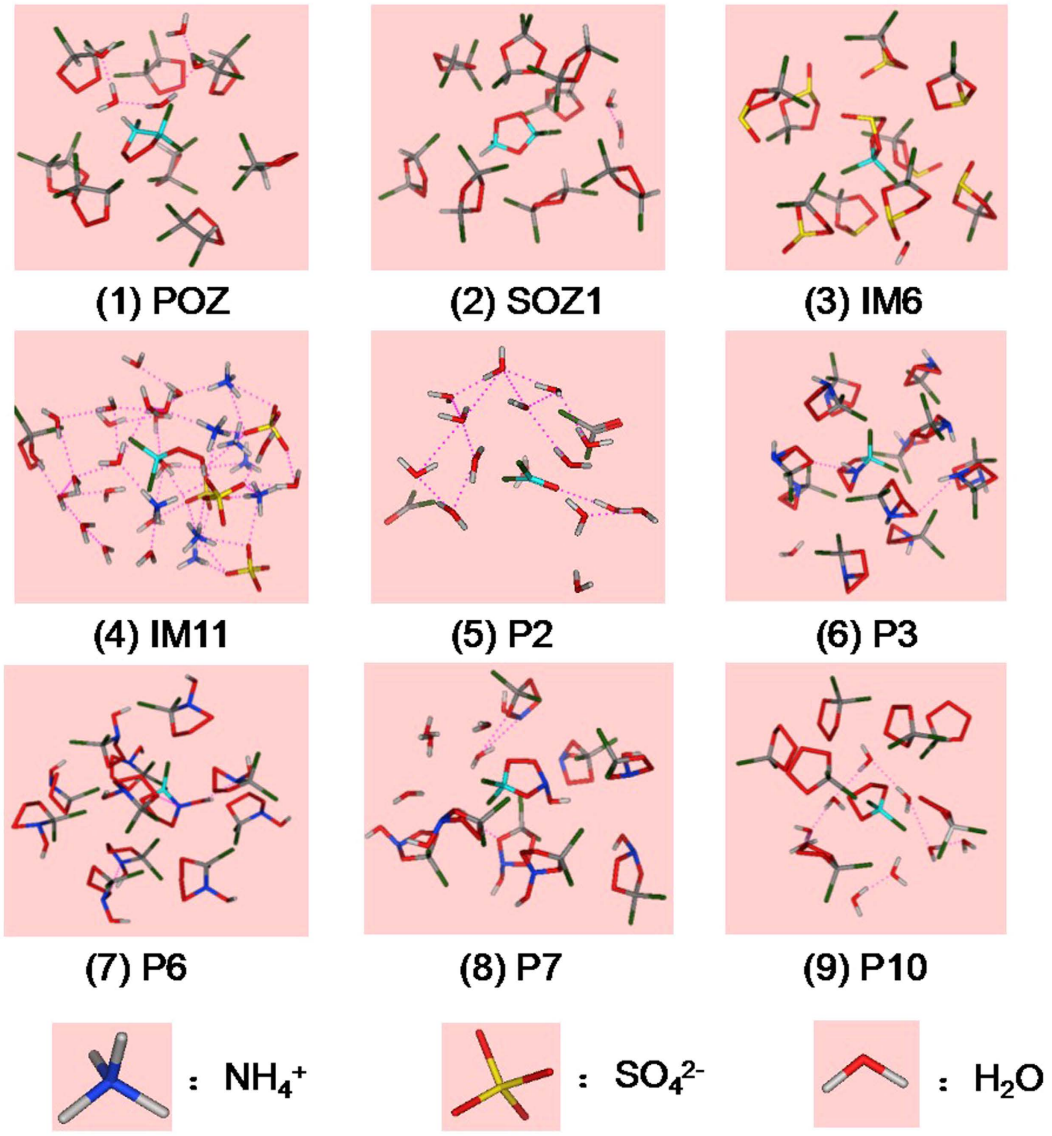

Figure 4. The binding mode of VOCs with other particles around 0.5 nm in the VOCs–$(NH_4)_2SO_4$-H_2O system.

2.25 nm. What accounts for this phenomenon is the appearance of hydration structures between SO_4^{2-}, NH_4^+ and H_2O.

The radial distribution function of other systems described above (see Supplementary Fig. S13-S20), respectively. The radial distribution functions of NH_4^+-SO_4^{2-}, NH_4^+-H_2O and SO_4^{2-}-H_2O between $(NH_4)_2SO_4$ and H_2O show the same trend in different systems, but the main difference exists in the radial distribution functions of OCs-OCs, OCs-SO_4^{2-} and OCs-H_2O which have different peaks.

The Binding mode and intermolecular force. The binding mode of SO_4^{2-} with other particles in distance of 0.45 nm in the POZ-$(NH_4)_2SO_4$-H_2O system is drawn in Fig. 3. With SO_4^{2-} as the center, a three-dimensional cage-like structure is formed with ammonium ion and water. The binding modes of different OCs are shown in Fig. 4. It is easy to see the distribution of different molecules around the center of OCs molecules. The water molecules are embedded in clusters of cyclic intermediates, for example, POZ, SOZ1, P3, P7, IM6, P6, and P10. As water soluble strong hydroxyl compounds, the IM11 can form the cluster with more water molecules, ammonium ion and sulfate ion. While P2 is mainly surrounded by water molecules. The forces between pairs of NH_4^+-SO_4^{2-}, NH_4^+-H_2O and SO_4^{2-}-H_2O are the charge electrostatic interaction, ion-induced and intermolecular hydrogen bonds. While the forces of OCs-OCs, OCs-SO_4^{2-}, OCs-H_2O are referred to as the dispersion forces between polar molecules, ion-induced and intermolecular hydrogen bonds. The binding energies between different particle-pairs in the OCs-$(NH_4)_2SO_4$-H_2O system are listed in Table 1.

The main driving force for the formation of clusters, *i.e.*, nucleation, should be the overall performance of charge electrostatic interaction, ion induced, dispersion forces, and intermolecular hydrogen bonds, and other

		(N)-(N)	(N)-SO_4^{2-}	(N)-NH_4^+	(N)-SO_4^{2-}	SO_4^{2-}-NH_4^+	SO_4^{2-}-H_2O	NH_4^+-H_2O
N = POZ	Coul	−1.95	0.12	−0.821	−322.25	−6638.72	−4780.76	−1430.39
	LJ	−257.54	−0.74	−1.021	−33.27	504.51	308.55	259.05
	Total	−259.49	−0.61	−1.85	−355.52	−6134.21	−4472.21	−1171.34
N = SOZ1	Coul	−12.09	0.02	−0.32	−287.54	−7429.56	−4251.53	−1134.95
	LJ	−306.11	−0.54	−0.53	−30.44	564.58	269.04	216.81
	Total	−318.20	−0.52	−0.85	−317.97	−6864.98	−3982.50	−918.15
N = IM6	Coul	6.98	−0.76	−4.49	−366.94	−6764.85	−4694.14	−1401.29
	LJ	−223.38	−3.01	−2.21	−34.31	517.36	302.64	250.92
	Total	−216.41	−3.77	−6.70	−401.25	−6247.50	−4391.50	−1150.36
N = IM11	Coul	−229.33	−561.45	59.48	−268.54	−7529.78	−3598.82	−1235.42
	LJ	−26.02	30.07	−17.69	−29.55	581.41	212.04	218.16
	Total	−255.35	−531.38	41.80	−298.09	−6948.36	−3386.78	−1017.25
N = P2	Coul	−0.32	1.52	−7.51	−228.49	−6976.61	−4568.74	−1329.28
	LJ	−13.82	−2.91	−2.11	−326.75	531.24	296.48	245.05
	Total	−14.14	−1.39	−9.62	−555.24	−6445.37	−4272.26	−1084.23
N = P3	Coul	−6.037	−6.92	−1.67	−368.16	−7394.28	−4200.27	−1207.29
	LJ	−139.74	−3.58	−2.88	−31.38	558.69	272.55	222.94
	Total	−145.78	−10.49	−4.54	−399.54	−6835.59	−3927.71	−984.35
N = P6	Coul	−41.06	−155.41	7.22	−541.53	−6701.71	−4603.05	−1416.98
	LJ	−162.66	5.54	−8.03	−320.49	515.50	293.80	257.93
	Total	−203.72	−149.86	−0.81	−862.02	−6186.22	−4309.25	−1159.06
N = P7	Coul	40.056	−180.96	14.84	−328.14	−6842.47	−4506.65	−1427.18
	LJ	−189.13	8.74	−6.21	−33.71	520.11	286.34	253.76
	Total	−149.07	−172.23	8.63	−361.85	−6322.37	−4220.31	−1173.42
N = P10	Coul	1.89	0.19	−0.65	−23.31	−6416.25	−4995.53	−1501.96
	LJ	−254.31	−1.13	−1.09	−252.82	497.22	319.19	268.40
	Total	−252.42	−0.94	−1.74	−276.14	−5919.04	−4676.34	−1233.56

Table 1. The binding energy (kCal/mol) between different pair-particle in the OCs-$(NH_4)_2SO_4$-H_2O system.

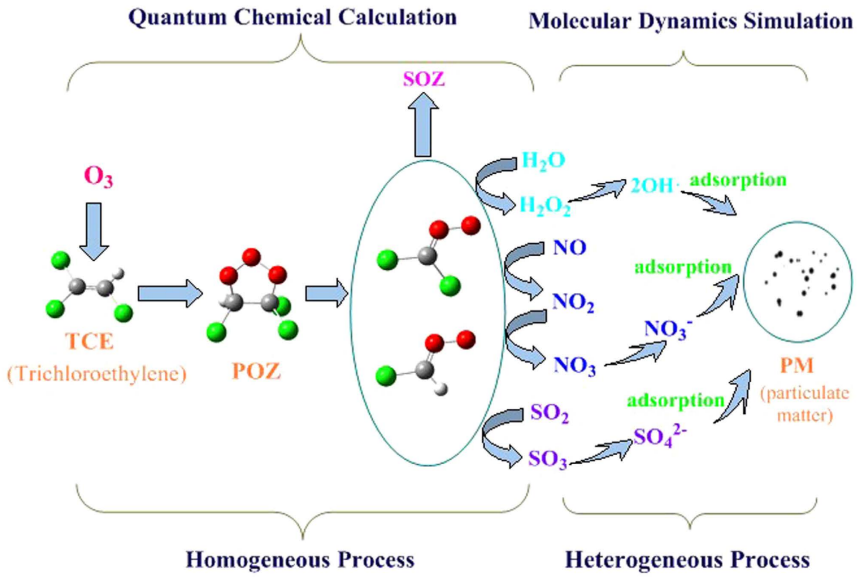

Figure 5. The schematic diagram from volatile organic compounds to the formation of new particle in the ozonation of trichloroethylene.

factors. The peak value of radial distribution function reflects the mutual attraction between the particles with nucleating ability. The higher the peak is, the easier the nucleation is. And the peak width of radial distribution

function is able to reflect the nucleus particle size. The wider the peak is, the bigger the size of the formation particle is.

Discussion

The Criegee radical generated in the ozonation of TCE can react with NO, NO_2, SO_2, H_2O, O_2 and other species in the atmosphere. During the oxidation process, the NO can be oxidized to NO_2 and then to NO_3, SO_2 can also be oxidized to SO_3, and then inorganic acid can be produced. In the presence of NH_3, inorganic salts $(NH_4)_2SO_4$ and NH_4NO_3 can be formed.

Apart from inorganic salts, the polar organic nitrogen and organic sulfur compounds, oxygen-containing heterocyclic intermediates and polyhydroxy compounds can be obtained too.

The polar organic intermediates, such as POZ, SOZ, organic nitrogen and organic sulfur compounds, oxygen-containing heterocyclic intermediates, and polyhydroxy compounds have their own tendency to aggregate to generate new fine particles and further produce the second organic aerosols in inorganic salt surface. The schematic diagram from volatile organic compounds to the formation of new particle in the ozonation of trichloroethylene is shown in Fig. 5.

Computational methods

Molecular Dynamic Simulation. The GROMACS 4.5.5 package with Amber99SB force field was used for all molecular dynamics simulations[36]. The GROMACS 4.5.5 package with Amber99SB force field was used for all molecular dynamics simulations[36]. The topology parameters of OCs were derived using RESP (Restrained Electro Static Potential) method with AM1-BCC model, which can create high quality atomic charges for organic molecules in polar solvent[37]. TIP3P model was used for water molecules. One OC molecule was placed in a box of 7 nm × 7 nm × 7 nm. Then 49 OCs, 50 SO_4^{2-}, 100 NH_4^+ and 5560 water molecules were inserted randomly into the box. Finally the system includes 50 OCs, 50 $(NH_4)_2SO_4$ and 5560 water molecules. Energy minimization and 100 ps NVT MD simulation were carried out to remove the steric clash. The subsequent 200 ps NPT MD simulation was done to adjust the box size and achieve reasonable density. Production MD simulation was performed for 2 ns at 300 K and the time step is 1 fs. PME (Particle Mesh Ewald) method was used to consider long-range electrostatic interactions. The last 500 ps trajectory was used in the following analyses.

References

1. Johnson, M. S. & Goodsite, M. E. Applications of theoretical methods to atmospheric science. *Advances in Quantum Chemistry* **55,** 1–4 (2008).
2. Hallquist, M. *et al.* The formation, properties and impact of secondary organic aerosol: current and emerging issues. *Atmospheric Chemistry and Physics* **9,** 5155–5236 (2009).
3. Kumar, M., Busch, D. H., Subramaniam, B. & Thompson, W. H. Criegee intermediate reaction with CO: mechanism, barriers, conformer-dependence, and implications for ozonolysis chemistry. *J Phys Chem A* **118,** 1887–94 (2014).
4. Criegee, R. Mechanism of ozonolysis. *Angewandte Chemie International Edition in English* **14,** 745–752 (1975).
5. Odum, J. R. *et al.* Gas/particle partitioning and secondary organic aerosol yields. *Environmental Science & Technology* **30,** 2580–2585 (1996).
6. Jang, M. & Kamens, R. M. Newly characterized products and composition of secondary aerosols from the reaction of α-pinene with ozone. *Atmospheric Environment* **33,** 459–474 (1999).
7. Koo, B., Ansari, A. S. & Pandis, S. N. Integrated approaches to modeling the organic and inorganic atmospheric aerosol components. *Atmospheric Environment* **37,** 4757–4768 (2003).
8. Volkamer, R. *et al.* Secondary organic aerosol formation from anthropogenic air pollution: Rapid and higher than expected. *Geophysical Research Letters* **33** (2006).
9. Rudich, Y., Donahue, N. M. & Mentel, T. F. Aging of organic aerosol: Bridging the gap between laboratory and field studies. *Annu. Rev. Phys. Chem.* **58,** 321–352 (2007).
10. Dzepina, K. *et al.* Evaluation of recently-proposed secondary organic aerosol models for a case study in Mexico City. *Atmospheric Chemistry and Physics* **9,** 5681–5709 (2009).
11. Zhu, C. *et al.* New Mechanistic Pathways for Criegee–Water Chemistry at the Air/Water Interface. *Journal of the American Chemical Society* **138,** 11164–11169 (2016).
12. Wang, G. *et al.* Persistent sulfate formation from London Fog to Chinese haze. *Proceedings of the National Academy of Sciences* **113,** 13630–13635 (2016).
13. Li, L. *et al.* Near-Barrierless Ammonium Bisulfate Formation via a Loop-Structure Promoted Proton-Transfer Mechanism on the Surface of Water. *Journal of the American Chemical Society* **138,** 1816–1819 (2016).
14. Stone, R. Counting the cost of London's killer smog. *Science* **298,** 2106–2107 (2002).
15. Parrish, D. D., Singh, H. B., Molina, L. & Madronich, S. Air quality progress in North American megacities: A review. *Atmospheric Environment* **45,** 7015–7025 (2011).
16. Pollack, I. B. *et al.* Trends in ozone, its precursors, and related secondary oxidation products in Los Angeles, California: A synthesis of measurements from 1960 to 2010. *Journal of Geophysical Research: Atmospheres* **118,** 5893–5911 (2013).
17. Parrish, D. D. & De Gouw, J. Synthesis of Policy Relevant Findings from the CalNex 2010 Field Study. https://www.esrl.noaa.gov/csd/projects/calnex/synthesisreport.pdf (2014).
18. Sun, Y. *et al.* Investigation of the sources and evolution processes of severe haze pollution in Beijing in January 2013. *Journal of Geophysical Research: Atmospheres* **119,** 4380–4398 (2014).
19. Wang, Y. *et al.* Mechanism for the formation of the January 2013 heavy haze pollution episode over central and eastern China. *Science China Earth Sciences* **57,** 14–25 (2014).
20. Guo, S. *et al.* Elucidating severe urban haze formation in China. *Proc Natl Acad Sci USA* **111,** 17373–8 (2014).
21. Zhang, R., Khalizov, A., Wang, L., Hu, M. & Xu, W. Nucleation and growth of nanoparticles in the atmosphere. *Chem Rev* **112,** 1957–2011 (2012).
22. Zhang, R. *et al.* Formation of urban fine particulate matter. *Chem Rev* **115,** 3803–55 (2015).
23. Seinfeld, J. H. & Pandis, S. N. *Atmospheric chemistry and physics: from air pollution to climate change* (John Wiley & Sons, 2016).
24. Zhang, R. *et al.* Chemical characterization and source apportionment of PM2.5 in Beijing: seasonal perspective. *Atmospheric Chemistry and Physics* **13,** 7053–7074 (2013).
25. Huang, B., Lei, C., Wei, C. & Zeng, G. Chlorinated volatile organic compounds (Cl-VOCs) in environment - sources, potential human health impacts, and current remediation technologies. *Environ Int* **71,** 118–38 (2014).

26. Kanakidou, M. *et al.* Organic aerosol and global climate modelling: a review. *Atmospheric Chemistry and Physics* **5,** 1053–1123 (2005).
27. Liu, F., Beames, J. M., Petit, A. S., McCoy, A. B. & Lester, M. I. Infrared-driven unimolecular reaction of CH3CHOO Criegee intermediates to OH radical products. *Science* **345,** 1596–1598 (2014).
28. Taatjes, C. A. *et al.* Direct measurements of conformer-dependent reactivity of the Criegee intermediate CH3CHOO. *Science* **340,** 177–180 (2013).
29. Welz, O. *et al.* Direct kinetic measurements of Criegee intermediate (CH2OO) formed by reaction of CH2I with O2. *Science* **335,** 204–207 (2012).
30. Su, Y.-T., Huang, Y.-H., Witek, H. A. & Lee, Y.-P. Infrared absorption spectrum of the simplest Criegee intermediate CH2OO. *Science* **340,** 174–176 (2013).
31. Drijvers, D., De Baets, R., De Visscher, A. & Van Langenhove, H. Sonolysis of trichloroethylene in aqueous solution: volatile organic intermediates. *Ultrasonics Sonochemistry* **3,** S83–S90 (1996).
32. Doucette, W. *et al.* Volatilization of trichloroethylene from trees and soil: measurement and scaling approaches. *Environ Sci Technol* **47,** 5813–20 (2013).
33. Andersin, J., Parkkinen, P. & Honkala, K. Pd-catalyzed hydrodehalogenation of chlorinated olefins: Theoretical insights to the reaction mechanism. *Journal of Catalysis* **290,** 118–125 (2012).
34. Nesnow, S. *et al.* Chemical carcinogens a review and analysis of the literature of selected chemicals and the establishment of the Gene-Tox carcinogen data base: A report of the US environmental protection agency Gene-Tox program. *Mutation Research/ Reviews in Genetic Toxicology* **185,** 1–195 (1987).
35. Prevention, P. TSCA Work Plan Chemical Risk Assessment Trichloroethylene: Degreasing, Spot Cleaning and Arts & Crafts Uses CASRN: 79-01-6. (2014).
36. Pronk, S. *et al.* GROMACS 4.5: a high-throughput and highly parallel open source molecular simulation toolkit. *Bioinformatics*, btt055 (2013).
37. Jakalian, A., Jack, D. B. & Bayly, C. I. Fast, efficient generation of high-quality atomic charges. AM1-BCC model: II. Parameterization and validation. *Journal of computational chemistry* **23,** 1623–1641 (2002).

Acknowledgements

This work is supported by National Natural Science Foundation of China (21277082, 21337001, 21577021, 21377028 and 21177025), Project for science and technology development of Shandong province (2014GSF117028), Program for New Century Excellent Talents in University (NCET-13-0349), Beijing National Laboratory for Molecular Science (20140160), and the Fundamental Research Funds of Shandong University (2015JC020). Strategic Priority Research Program (B) of the Chinese Academy of Sciences, Grant (No. XDB05010200). We also appreciate Dr. Fancui Meng's technical support and Professor Hurtmut Hermann's constructive suggestion.

Author Contributions

N.W. and X.M.S. designed and performed the mechanism calculations and molecular dynamic simulation, J.M.C. and X.L. performed the integrative data analysis, and then wrote the manuscript. All authors discussed the results and commented on the paper.

Additional Information

Supplementary information accompanies this paper at http://www.nature.com/srep

Competing financial interests: The authors declare no competing financial interests.

How to cite this article: Wang, N. *et al.* Heterogeneous Nucleation of Trichloroethylene Ozonation Products in the Formation of New Fine Particles. *Sci. Rep.* **7**, 42600; doi: 10.1038/srep42600 (2017).

Publisher's note: Springer Nature remains neutral with regard to jurisdictional claims in published maps and institutional affiliations.